THE JOURNAL OF BIOLOGICAL CHEMISTRY VOL. 283, NO. 14, pp. 9231–9238, April 4, 2008

A Role for IOP1 in Mammalian Cytosolic Iron-Sulfur Protein Biogenesis*[S]

Received for publication, September 27, 2007, and in revised form, February 7, 2008 Published, JBC Papers in Press, February 12, 2008, DOI 10.1074/jbc.M708077200

Daisheng Song and Frank S. Lee[1]

From the Department of Pathology and Laboratory Medicine, University of Pennsylvania School of Medicine, Philadelphia, Pennsylvania 19104

The biogenesis of cytosolic iron-sulfur (Fe-S) proteins in mammalian cells is poorly understood. In *Saccharomyces cerevisiae*, there is a pathway dedicated to cytosolic Fe-S protein maturation that involves several essential proteins. One of these is Nar1, which intriguingly is homologous to iron-only hydrogenases, ancient enzymes that catalyze the formation of hydrogen gas in anaerobic bacteria. There are two orthologues of Nar1 in mammalian cells, iron-only hydrogenase-like protein 1 (IOP1) and IOP2 (also known as nuclear prelamin A recognition factor). We examined IOP1 for a potential role in mammalian cytosolic Fe-S protein biogenesis. We found that knockdown of IOP1 in both HeLa and Hep3B cells decreases the activity of cytosolic aconitase, an Fe-S protein, but not that of mitochondrial aconitase. Knockdown of IOP2, in contrast, had no effect on either. The decrease in aconitase activity upon IOP1 knockdown is rescued by expression of a small interference RNA-resistant version of IOP1. Upon loss of its Fe-S cluster, cytosolic aconitase is known to be converted to iron regulatory protein 1, and consistent with this, we found that IOP1 knockdown increases transferrin receptor 1 mRNA levels and decreases ferritin heavy chain protein levels. IOP1 knockdown also leads to a decrease in activity of xanthine oxidase, a distinct cytosolic Fe-S protein. Taken together, these results provide evidence that IOP1 is involved in mammalian cytosolic Fe-S protein maturation.

Iron-sulfur (Fe-S)[2] proteins play an essential role in multiple physiologic processes, including electron transport, enzyme catalysis, and regulation of gene expression (1). Among the most studied of these proteins are those involved in mitochondrial oxidative phosphorylation, but it is clear that these proteins are present in other cellular compartments, including the cytoplasm and nucleus. The synthesis and maturation of Fe-S proteins in eukaryotes is complex, and much of our current understanding of this pathway derives from studies in yeast (2). The central elements of this pathway are as follows. The cysteine desulfurase Nfs1 (also known as IscS) removes sulfur from the amino acid cysteine. This sulfur is then combined with iron to form Fe-S clusters. These clusters, which can take on many forms, including [2Fe-2S] and [4Fe-4S] clusters, are then combined with apoproteins, resulting in Fe-S proteins. The initial steps of the pathway, including the desulfuration of cysteine and assembly of Fe-S clusters, occur within the mitochondrion. Thus, defects in mitochondrial Fe-S assembly impact Fe-S proteins not only in the mitochondrion but also in the cytosol. The Fe-S clusters are then transported to the appropriate compartments for subsequent assembly of the mature Fe-S proteins. A substantial amount is known about the initial steps. Less is known of the compartment-specific assembly. In yeast, a cytoplasmic iron-sulfur protein assembly pathway has been characterized (3). This pathway comprises at least four distinct proteins: cytosolic Fe-S cluster-deficient 1 (Cfd1), nucleotide-binding protein of 35 kDa (Nbp35), cytoplasmic iron-sulfur protein assembly 1 (Cia1), and Nar1 (4–7). Genetic deletion of these components leads to lethality and impairment of Fe-S protein assembly in the cytosol, but not in the mitochondrion. Various components, in addition, interact physically. For example, Cfd1 interacts with Nbp35, while Cia1 interacts with Nar1 (6, 8).

Even less is known of the cytoplasmic Fe-S assembly pathway in mammals (9). Knockdown studies employing siRNA identify a role for NFS1 in cytoplasmic as well as mitochondrial Fe-S assembly, presumably through a role analogous to that in yeast in catalyzing desulfuration of cysteine (10, 11). Consistent with this, mammalian NFS1 is enzymatically active as a cysteine desulfurase (12). Other studies indicate an important role for cytosolic versions of otherwise predominantly mitochondrial proteins in cytosolic Fe-S protein maturation. Thus, the cytosolic form of the scaffold protein ISCU, produced by alternative splicing, is necessary for the maturation of cytosolic aconitase, which is an Fe-S protein (13). Alternative splicing also produces a cytosolic form of another scaffold protein NFU (14), raising the possibility that a similar situation may apply to this protein (9). These findings in turn suggest that the mammalian cytosolic Fe-S protein pathway may differ in certain fundamental respects from that in yeast. It therefore begs the question of whether proteins dedicated to the Fe-S protein pathway in yeast exist in mammalian cells, and if so, whether they serve homologous functions in mammalian cells.

With regard to Nar1, there are in fact two orthologues in mammalian cells, IOP1 and IOP2 (also known as nuclear prel-

* This work was supported by National Institutes of Health Grant R01-GM71459. The costs of publication of this article were defrayed in part by the payment of page charges. This article must therefore be hereby marked "*advertisement*" in accordance with 18 U.S.C. Section 1734 solely to indicate this fact.

[S] The on-line version of this article (available at http://www.jbc.org) contains supplemental Figs. S1–S3.

[1] To whom correspondence should be addressed: Dept. of Pathology and Laboratory Medicine, University of Pennsylvania School of Medicine, 605 Stellar Chance Laboratories, 422 Curie Blvd., Philadelphia, PA 19104. Tel.: 215-898-4701; Fax: 215-573-2272; E-mail: franklee@mail.med.upenn.edu.

[2] The abbreviations used are: Fe-S, iron-sulfur; DFO, desferrioximine; HA, hemagglutinin; HIF, hypoxia-inducible factor; HPRT, hypoxanthine-guanine phosphoribosyltransferase; IRE, iron-response element; IRP, iron regulatory protein; UTR, untranslated region; siRNA, small interference RNA.

amin A recognition factor (Narf)) (15, 16). We initially identified IOP1 (15) as a predominantly cytoplasmic protein that modulates the activity of hypoxia-inducible factor-1α, a transcription factor that is a master regulator of cellular responses to low oxygen tension (17). IOP1, like Nar1, shows conservation of cysteine residues that, in bacterial iron-only hydrogenases, are involved in chelating a distinctive active site Fe-S cluster known as the H-cluster. However, like Nar1, IOP1 does not display hydrogenase activity. Based on its homology to Nar1, we hypothesized that IOP1 might play a role in cytosolic Fe-S protein maturation. We found that siRNA knockdown of IOP1 results in decreased cytosolic, but not mitochondrial, aconitase activity. In parallel experiments knocking down IOP2, which was originally identified based on its capacity to bind to prenylated prelamin A, there was no effect on either activity. IOP1 knockdown also decreases the activity of xanthine oxidase, a distinct Fe-S protein. We conclude that IOP1 does indeed play a role in cytoplasmic Fe-S protein biogenesis in mammalian cells.

EXPERIMENTAL PROCEDURES

Cell Culture, Transfection, and Extract Preparation—HeLa and Hep3B cells were obtained from ATCC and grown in Dulbecco's modified Eagle's medium supplemented with 10% (v/v) fetal bovine serum, 100 units/ml penicillin, and 100 μg/ml streptomycin. For stable transfection, 1000 μg/ml of G418 was also included and resistant clones selected 14 days after transfection. For transient transfection, cells were typically seeded in 6-well or 10-cm plates for siRNA experiments or in 24-well plates for luciferase assays. Lipofectamine 2000 (Invitrogen) was employed for transfections. For siRNA experiments, cells were transfected on days 0, 3, and 6 and the final siRNA concentration was 20 nM; cells were harvested on day 9. For luciferase measurements, cells were cotransfected with firefly and *Renilla* luciferase (pRL-TK) reporter constructs on day 7; cells were then lysed 48 h after transfection of luciferase reporter constructs in passive lysis buffer (Promega). To prepare extracts for all other enzymatic assays, cells were resuspended in 100 mM Hepes, pH 7.4, containing 0.25 M sucrose, 0.01% digitonin, and mammalian cell extract protease inhibitor mixture (Sigma) essentially as described (11) with minor modifications. After 10 min on ice, the suspension was centrifuged at 10,000 $\times$ *g* for 10 min at 4 °C. The supernatant was designated the cytosolic fraction. The cell pellets were further washed three times in 100 mM Hepes, pH 7.4, containing 0.25 M sucrose, with a 1-min centrifugation at 3,000 $\times$ *g* after each wash. The resulting pellet was then lysed in 100 mM Hepes, pH 7.4, containing 0.5% Triton X-100 and mammalian cell extract protease inhibitor mixture. After 10 min on ice, the lysate was centrifuged at 10,000 $\times$ *g* for 10 min at 4 °C. The supernatant from this centrifugation was designated the mitochondrial fraction. This fraction also contains nuclear proteins and was examined for IOP2 levels by Western blotting. Cytosolic and mitochondrial extracts were either tested for enzymatic activity immediately or aliquoted and stored at −80 °C for later assay. Protein concentrations of extracts were measured using a DC Protein Assay kit (Bio-Rad). For Western blotting of whole cell lysates, the lysates were prepared as described (18).

siRNA, Plasmids, and Chemicals—siRNA duplexes were synthesized by Dharmacon. The sequences of oligonucleotides employed to prepare siRNA duplexes targeting IOP1 (IOP1-A) and control siRNA (Control-B) have been described (15). The sequences of oligonucleotides employed to prepare other siRNA duplexes were as follows. IOP2-A, GCACACAUCUUCAGACAUGUU and CAUGUCUGAAGAUGUGUGCUU; IOP2-B, GAACGGAGAGGUGGUGUUAUU and UAACACCACCUCUCCGUUCUU; NFS1, CAAGUAGCAUCUCUGAUUGUU and CAAUCAGAGAUGCUACUUGUU. pcDNA3-HA-IOP1^R, which encodes for an IOP1 cDNA resistant to IOP1-A siRNA due to three nucleotide changes in the siRNA target sequence, has been described previously (15). pIRE3-Luc, which contains the transferrin receptor-1 (TfR1) 3′-iron-response element (IRE) downstream of the luciferase coding sequence, was constructed by amplifying by PCR the TfR1 IRE using IMAGE clone 4660895 (ATCC) as a template and the following two primers, 5′-TTAGTCTAGAGCTTTCTGTCCTTTTGG-3′ and 5′-ACGTTCTAGAAGCTTTGAAGATGTCATTGC-3′. The resulting 0.7-kb PCR product was digested with XbaI, subcloned into the XbaI site pGL3promoter (Promega) to yield pIRE3-Luc. pBS-IRE5-Luc, which contains the ferritin heavy chain 5′-IRE upstream of the luciferase coding sequence, was constructed by first subcloning into the SfiI/HindIII site of pGL3promoter a duplex comprised of the following two oligonucleotides, 5′-CGGCCTCTGAGCTATTCCAGAATTCGTCGGGGTTTCCTGCTTCAACAGTGCTTGGACGGAACCCGGCGCA-3′ and 5′-AGCTTGCGCCGGGTTCCGTCCAAGCACTGTTGAAGCAGGAAACCCCGACGAATTCTGGAATAGCTCAGAGGCCGAGG-3′. The 1.8-kb EcoRI(blunt)/XbaI band from the resulting product was then subcloned into the KpnI(blunt)/XbaI site of pBS SK to create pBS-IRE5-Luc.

pcDNA3-FLAG-IRP1 was constructed as follows. First, the 2.9-kb BamH I/HindIII (blunt) fragment of IMAGE clone 3915517 (ATCC) was subcloned into the BamHI/XbaI (blunt) site of pcDNA3-HA. Into the NheI/BamHI site of the product was cloned a duplex comprised of the following two oligonucleotides, 5′-CTAGCAGATCTGGGATCCAGATGAGCAACCCATTCGCACACCTTGCTGAGCCATTA-3′ and 5′-GATCTAATGGCTCAGCAAGGTGTGCGAATGGGTTGCTCATCTGGATCCCAGATCTG-3′ to yield pcDNA3-HA-IRP1. The latter was digested with BamH I and XbaI, and the 2.9-kb product was then subcloned into the BamH I/XbaI site of pcDNA3-FLAG to yield pcDNA3-FLAG-IRP1. Constructs were sequenced to confirm their authenticity. Chemicals were from Sigma unless otherwise stated.

Antibodies and Western Blotting—Polyclonal antibodies to glutathione *S*-transferase-IOP1-(417–476) were raised in rabbits and affinity-purified on maltose-binding protein IOP1-(417–476) conjugated to agarose (Covance Research Products). Polyclonal antibodies to maltose-binding protein-IOP2-(382–456) were raised in rabbits and affinity-purified on glutathione *S*-transferase IOP2-(382–456) conjugated to agarose (Alpha Diagnostic). Other antibodies employed were anti-HIF-1α (Clone 54; BD Biosciences), anti-FLAG (M2; Sigma), and anti-NFS1 (ARP33115 T100; Aviva Systems). The follow-

ing antibodies were from Santa Cruz Biotechnology: anti-ferritin heavy chain (H-53), anti-cytochrome *c* (7H8), anti-IRP1 (H-64), anti-IRP2 (7H6), anti-HA (F-7), anti-actin (C-2), and anti-β-tubulin (H-235). Western blotting was performed as described (18). Typically, 30 μg of cell lysate were subjected to SDS-PAGE and the proteins transferred to polyvinylidene difluoride membranes. The membranes were blocked with 10% nonfat milk in phosphate-buffered saline containing 0.05% Tween 20 and probed with the relevant antibodies followed by horseradish peroxidase-coupled secondary antibodies. Detection was performed using SuperSignal substrate (Pierce).

Enzyme Assays—The activities of firefly and *Renilla* luciferase were measured using a Dual Luciferase Reporter system (Promega) and a Wallach LB9507 luminometer. Firefly luciferase activity was normalized to that of *Renilla* luciferase. For all other enzymatic activities, equal quantities of extracts as assessed by protein concentration were assayed. Aconitase activity in extracts was measured by activity against 2 mM cis-aconitate in the presence of 1 mM $MnSO_4$, 0.2 mM NADP, and 0.4 unit/ml of porcine heart isocitrate dehydrogenase (Sigma) using degassed buffer at 25 °C (19). The reduction of NADP was measured by changes in absorbance at 340 nm. Citrate synthase activity was measured by activity toward 0.5 mM oxaloacetate in the presence of 100 mM Tris, pH 8.0, 0.5 mM acetyl-CoA, and 0.5 mM 5,5′-dithio-bis(2-nitrobenzoic acid). The reduction of 5,5′-dithio-bis(2-nitrobenzoic acid) was monitored by changes in absorbance at 412 nm (10). Lactate dehydrogenase activity was determined by activity against 0.66 mM sodium pyruvate in the presence of 100 mM Hepes, pH 7.6, and 0.13 mM NADH at 25 °C. Oxidation of NADH was measured by the change of absorbance at 340 nm (20). Glucose-6-phosphate dehydrogenase activity was determined against 3.3 mM glucose-6-phosphate in the presence of 50 mM Tris, pH 7.8, 3 mM $MgCl_2$, and 0.2 mM NADP at 25 °C. Reduction of NADP was measured by changes in absorbance at 340 nm. Xanthine oxidase activity was determined using the Amplex Red xanthine/xanthine oxidase assay kit (Invitrogen) according to the manufacturer's protocol. Absorbance changes were measured at 570 nm at 37 °C.

Protein Synthesis Assay—HeLa cells in 24-well plates were incubated in methionine-free Dulbecco's modified Eagle's medium containing 10% dialyzed fetal bovine serum and 10 μCi of [^{35}S]Met/well for 1 h. Cells were lysed and then radiolabeled proteins precipitated with trichloroacetic acid essentially as described (21). [^{35}S]Met incorporation was measured by scintillation counting and normalized to the protein concentration of the cell lysate.

Iron Regulatory Protein (IRP) Electrophoretic Mobility Shift Assay—pBS-IRE5-Luc was linearized by digestion with HindIII and employed as a template for *in vitro* transcription using T7 RNA polymerase in the presence of [^{32}P]UTP. Radiolabeled probe was purified by denaturing PAGE and incubated for 20 min at 25 °C with cytoplasmic extracts in 100 mM Hepes, pH 7.4, containing 3 mg/ml heparin, and electrophoretic mobility shift assays were performed essentially as described (22) in 0.5× Tris borate-EDTA buffer. In some cases, β-mercaptoethanol was included in the incubation to a final concentration of 2%. For the IRP1-positive control, COS-7 cells were transfected with pcDNA3-FLAG-IRP1. IRP1 was then immunoprecipitated with anti-FLAG (M2) antibodies and eluted with 3× FLAG peptide (Sigma). For the IRP2-positive control, IRP2 was immunoprecipitated from HeLa cells with anti-IRP2 antibodies and eluted with 4% β-mercaptoethanol (23).

Real-time PCR—Total RNA was extracted from cells using TRIzol® reagent (Invitrogen). Reverse transcription reactions to produce cDNA were performed using a Hi Capacity cDNA synthesis kit (ABI). Real-time PCR reactions were performed on 20-ng equivalents of cDNA using SYBR Green Master mix (ABI) and an ABI 7300 real-time PCR machine. The PCR cycling conditions were as follows: 50 °C for 2 min and 95 °C for 10 min followed by 40 PCR cycles (95 °C for 15 s, 60 °C for 1 min). The following oligonucleotides were employed as primers. hNFS1 forward (F), ACTCCCGGACACATGCTTATG; hNFS1 reverse (R), GCTGACGAGCACGTTCCAT; hIOP2 F, GGCGCTGACTGCGTGTTAA; hIOP2 R, AGGTCACCTTGCTCCATTATTTG. hFerritin-H F, TGGGAGCGCCCGAAT; hFerritin-H R, CCCAGGGTGTGCTTGTCAA; hTfR1 F, GTGACCCTTACACACCTGGATTC; hTfR1 R, TGATGACCGAGATGGTGGAA; hHPRT F, CGTCTTGCTCGAGATGTGATG; hHPRT R, GCACACAGAGGGCTACAATGTG. The sequences of the β-actin primers have been previously described (15). Dissociation curve analysis for each set of probes revealed single peaks. Relative quantification was performed employing the $\Delta\Delta C_t$ method and β-actin as the endogenous control.

Statistical Analysis—Student's *t* test and analysis of variance were used for statistical analysis. Significant differences were considered when $p < 0.05$.

RESULTS

In initial experiments to assess whether IOP1 might be involved in cytosolic Fe-S protein biogenesis, we employed an siRNA approach in HeLa cells. We employed a synthetic siRNA to IOP1 that we have previously shown to be effective in both Hep3B and human embryonic kidney 293 cells (15), and as shown in Fig. 1*A*, this siRNA is also effective in knocking down IOP1 in HeLa cells (compare *lanes 1* and *2*). We also employed an siRNA to NFS1, because previous studies have shown that NFS1 knockdown leads to strong impairment of cytosolic as well as mitochondrial Fe-S protein biogenesis (10, 11). As shown in Fig. 1, *B* and *C*, this siRNA effectively reduces NFS1 protein levels as assessed by Western blot and NFS1 mRNA levels as assessed by real-time PCR, and it may also be noted that it does not have an effect on IOP1 protein levels (Fig. 1*A*). We then transfected HeLa cells with three rounds of these siRNAs, as well as a nontargeting control siRNA, at intervals of 3 days. At 9 days after the initial transfection, we prepared cytosolic and mitochondrial extracts and measured activities of various enzymes in these extracts.

We first measured cytosolic aconitase, a well characterized Fe-S protein that interconverts citrate to isocitrate. As shown in Fig. 1*D*, we found that IOP1 knockdown reduces activity to 58 ± 8% of that of control, comparable with the reduction to 51 ± 12% observed upon NFS1 siRNA treatment ($p < 0.01$ for both). We note that these decreases were not apparent after 3 days of knockdown of either IOP1 or NFS1, and others have made similar observations with NFS1 (10). We also measured

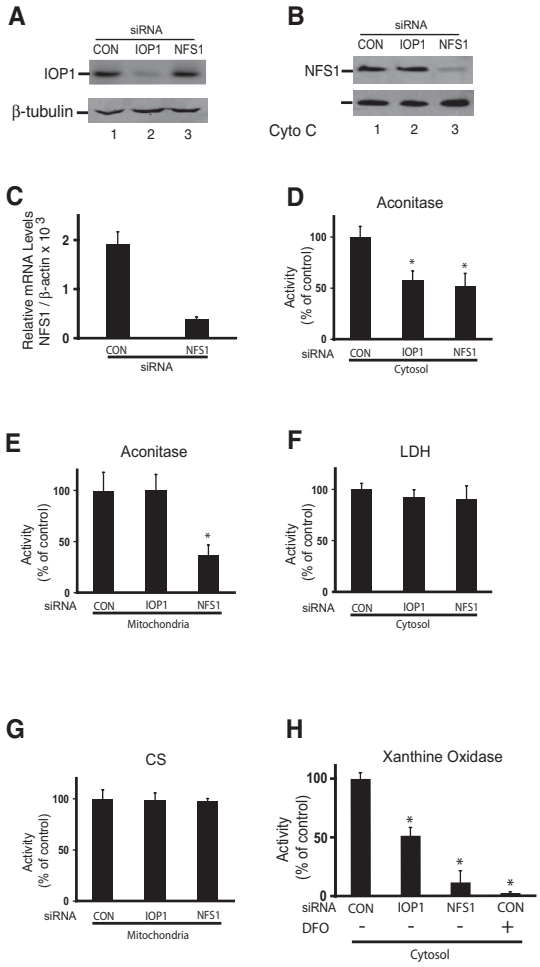

FIGURE 1. **Effects of IOP1 knockdown on aconitase and xanthine oxidase activities in HeLa cells.** HeLa cells were transfected with the indicated siRNAs. *A*, total cellular extracts (20 μg) were analyzed by Western blotting using antibodies against IOP1 or β-tubulin. *B*, mitochondrial extracts (10 μg) were analyzed by Western blotting using antibodies against NFS1 or cytochrome *c*. *C*, total RNA was isolated from cells and analyzed by real-time PCR for NFS1 mRNA (means ± S.D.) and normalized to that of β-actin. The level of NFS1 mRNA upon NFS1 knockdown is 21% of that of control. *D–G*, cytosolic or mitochondrial extracts were assayed for aconitase, lactate dehydrogenase (*LDH*), or citrate synthase (*CS*) activity as indicated. Shown are the means ± S.D., $n = 3$. *, $p < 0.01$. *H*, cytosolic extracts were assayed for xanthine oxidase activity. Some cells were also treated with 100 μM DFO for 20 h prior to harvest, as indicated. Shown are the means ± S.D., $n = 3$. *, $p < 0.01$.

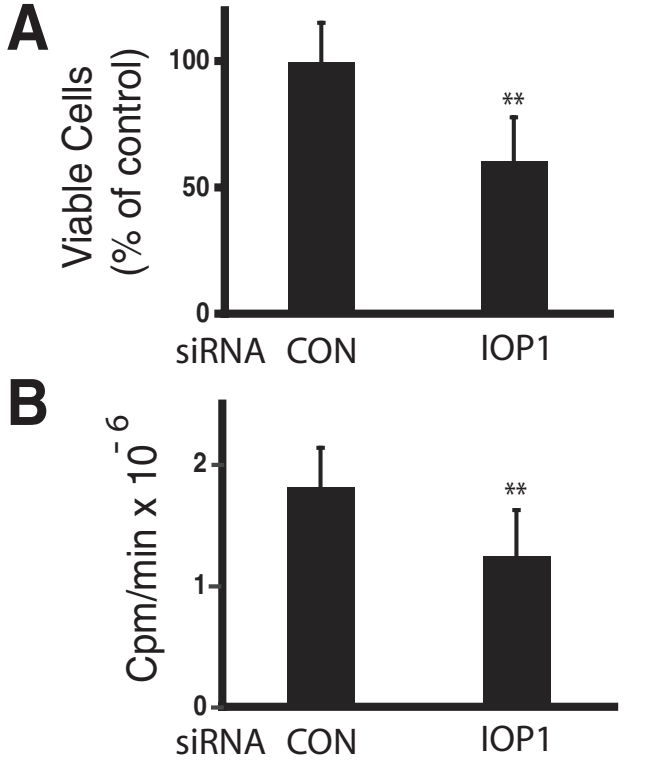

FIGURE 2. **Effects of IOP1 knockdown on cell viability and global protein synthesis in HeLa cells.** HeLa cells were transfected with the indicated siRNAs. *A*, HeLa cells were counted by trypan blue exclusion after 9 days. Shown are the means ± S.D., $n = 3$. **, $p < 0.05$. *B*, HeLa cells were assayed for protein synthesis at 9 days by labeling with [^{35}S]Met followed by trichloroacetic acid precipitation. **, $p <= 0.05$.

mitochondrial aconitase, which is an Fe-S enzyme distinct from cytosolic aconitase. NFS1 knockdown reduced mitochondrial aconitase activity to 36 ± 10% of control, consistent with an essential function in both mitochondrial and cytosolic Fe-S protein maturation (Fig. 1*E*). In contrast, IOP1 knockdown was without effect on mitochondrial aconitase activity. In control experiments, we assayed for activities of three non-Fe-S proteins, cytosolic lactate dehydrogenase, mitochondrial citrate synthase, and cytosolic glucose-6-phosphate dehydrogenase. As shown in Fig. 1, *F* and *G*, and supplemental Fig. 1, respectively, neither IOP1 nor NFS1 knockdown had effects on the activities of these enzymes. These enzymes are markers of their respective cellular compartments, and in additional experiments we found that the level of lactate dehydrogenase activity measured in the mitochondrial fraction was 3% of that in the cytosolic fraction, whereas the level of citrate synthase activity measured in the cytosolic fraction was 9% of that in the mitochondrial fraction (data not shown), indicative of effective separation of the two compartments. These experiments therefore provide initial evidence for IOP1 playing a role in cytosolic, but not mitochondrial, Fe-S protein biogenesis.

We next examined effects of IOP1 knockdown on a distinct cytosolic Fe-S protein, xanthine oxidase. HeLa cells were treated with IOP1, NFS1, or control siRNA and then xanthine oxidase activity measured in extracts. We employed two positive controls. One was desferrioxime (DFO), which essentially abolishes measurable xanthine oxidase activity. The other was NFS1. Under conditions where NFS1 knockdown reduces xanthine oxidase levels to 12 ± 9%, we found that IOP1 knockdown reduces it as well, to 51 ± 7% ($p < 0.01$) (Fig. 1*H*). This therefore provides evidence that IOP1 knockdown impairs the biogenesis of at least two distinct cytosolic Fe-S proteins.

NFS1 knockdown in mammalian cells was previously reported to lead to growth impairment (10). Upon IOP1 knockdown, we made a similar observation, with 61% viable cells compared with control following 9 days of siRNA treatment ($p < 0.05$) (Fig. 2*A*). Deletion of Nar1 in *Saccharomyces cerevisiae* is lethal, and it has been linked to the maturation of Rli1p, an essential cytosolic Fe-S protein required for ribosome biogenesis (24, 25). We therefore examined whether IOP1 knockdown affects global protein synthesis. As assessed by [^{35}S]Met incorporation, we found that IOP1 knockdown does indeed decrease global protein synthesis to 68% of that of control ($p < 0.05$ (Fig. 2*B*)).

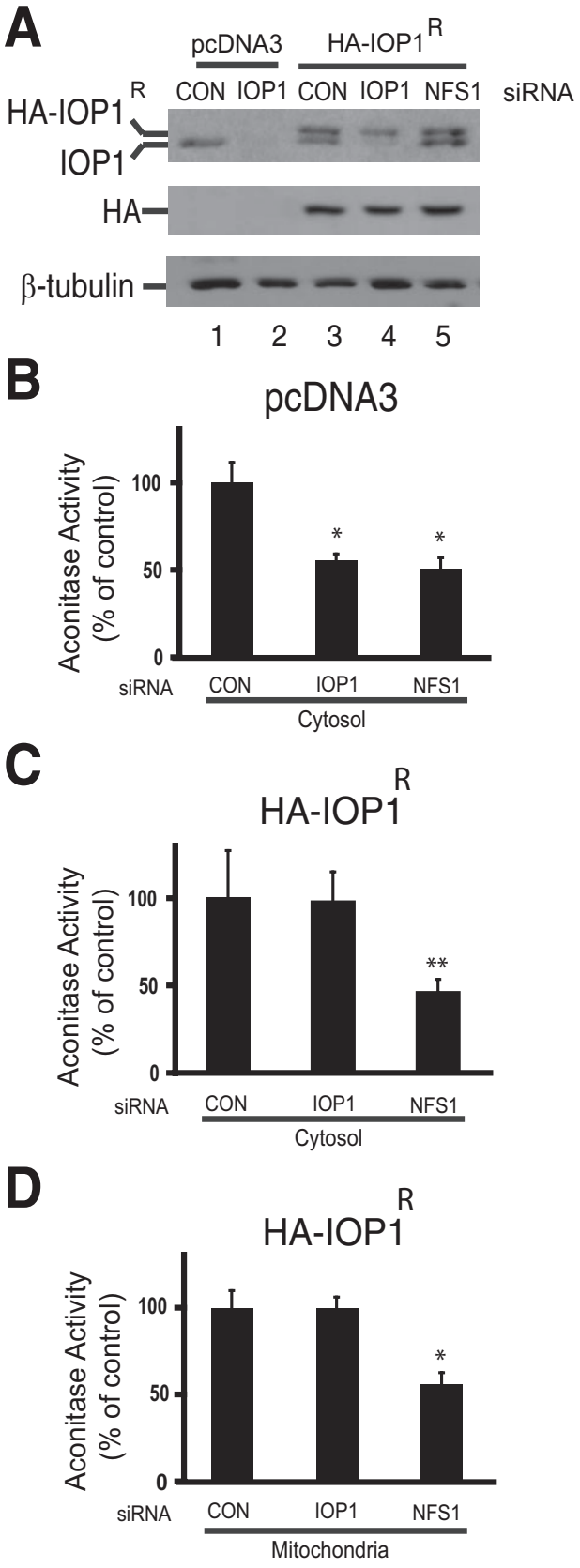

FIGURE 3. **Rescue of IOP1 knockdown effect by siRNA-resistant IOP1.** HeLa cells stably transfected with pcDNA3 or pcDNA3-HA-IOP1^R were transfected with the indicated siRNAs. *A*, total cellular extracts (30 μg) were analyzed by Western blotting using antibodies against IOP1 (*upper panel*), the HA tag (*middle panel*), or β-tubulin (*lower panel*). The positions of endogenous IOP1 and the stably expressed HA-IOP1^R are as indicated. *B–D*, cytosolic or mitochondrial extracts were assayed for aconitase activity as indicated. Shown are the means $\pm$ S.D., $n = 3$. *, $p < 0.01$; **, $p < 0.05$.

We examined a different cell line, Hep3B. In analogous experiments, we found that IOP1 knockdown reduced cytosolic aconitase activity to 54 $\pm$ 5% of that of control, again similar to the effect seen with NFS1 knockdown in this cell line (59 $\pm$ 4%, $p < 0.01$ for both, supplemental Fig. S2*A*). Under conditions in which NFS1 knockdown reduced mitochondrial aconitase activity to 52 $\pm$ 7% of control, we found no effect of the IOP1 siRNA (supplemental Fig. S2*B*). Both siRNAs, in addition, were without effect on cytosolic lactate dehydrogenase and citrate synthase activities (supplemental Fig. 2, *C* and *D*, respectively). Lactate dehydrogenase and citrate synthase activities measured in the mitochondrial and cytosolic fractions, respectively, were in this cell line, 9 and 10% of that measured in the cytosolic and mitochondrial fractions, respectively, again indicating efficient fractionation. As expected, the IOP1 siRNA was effective in reducing IOP1 protein levels, and we observed increased HIF-1α protein levels (data not shown), as we have reported previously (15). Interestingly, NFS1 did not affect HIF-1α protein levels (data not shown). IOP1 knockdown decreased viability in these cells as well (supplemental Fig. S2*E*).

To provide further evidence for the specificity of the IOP1 knockdown effect, we generated HeLa cell lines stably transfected with either an expression vector for siRNA-resistant, HA-tagged IOP1 (denoted HA-IOP1^R) or as a control, empty vector (pcDNA3). As shown in Fig. 3*A*, the HA-IOP1^R appears as a more slowly migrating species compared with endogenous IOP1 upon SDS-PAGE. It is also immunoreactive against anti-HA antibodies, as expected. Importantly, IOP1 siRNA treatment knocks down endogenous IOP1 protein levels in both HA-IOP1^R and control cell lines (Fig. 3*A*, *upper panel*, *lanes 4* and *2*, respectively) without affecting HA-IOP1^R protein levels. When we assayed cytosolic and mitochondrial aconitase activity in these two cell lines, we found that expression of the siRNA-resistant IOP1 reverses the IOP1 siRNA-induced decrease in cytosolic aconitase activity (Fig. 3, *B* and *C*, compare *middle columns*). As a control, NFS1 siRNA continued to be effective in decreasing cytosolic aconitase activity in both cell lines, as well as mitochondrial aconitase activity in the HA-IOP1^R-expressing cell line (Fig. 3*D*).

A homologue of IOP1, IOP2, exists in mammalian cells. To determine whether IOP2 might also play a role in cytosolic Fe-S protein biogenesis, we examined the effects of two IOP2 siRNAs, each targeting a distinct region of the IOP2 coding sequence. As shown in Fig. 4*A*, both were effective in diminishing IOP2 mRNA levels (IOP2-A to 13% and IOP-B to 11% of control). Both also decreased IOP2 protein levels (Fig. 4*B*). We next transfected HeLa cells with these siRNAs, a negative control siRNA, or as a positive control, the IOP1 siRNA. We found that under conditions in which the latter diminishes cytosolic aconitase activity, no significant effects are seen with either of the IOP2 siRNAs (Fig. 4*C*). In addition, the IOP2 siRNA did not affect mitochondrial aconitase activity, similar to the result obtained with IOP1 siRNA (Fig. 4*D*). We also treated cells with the iron chelator DFO for 20 h, and as one might predict, this

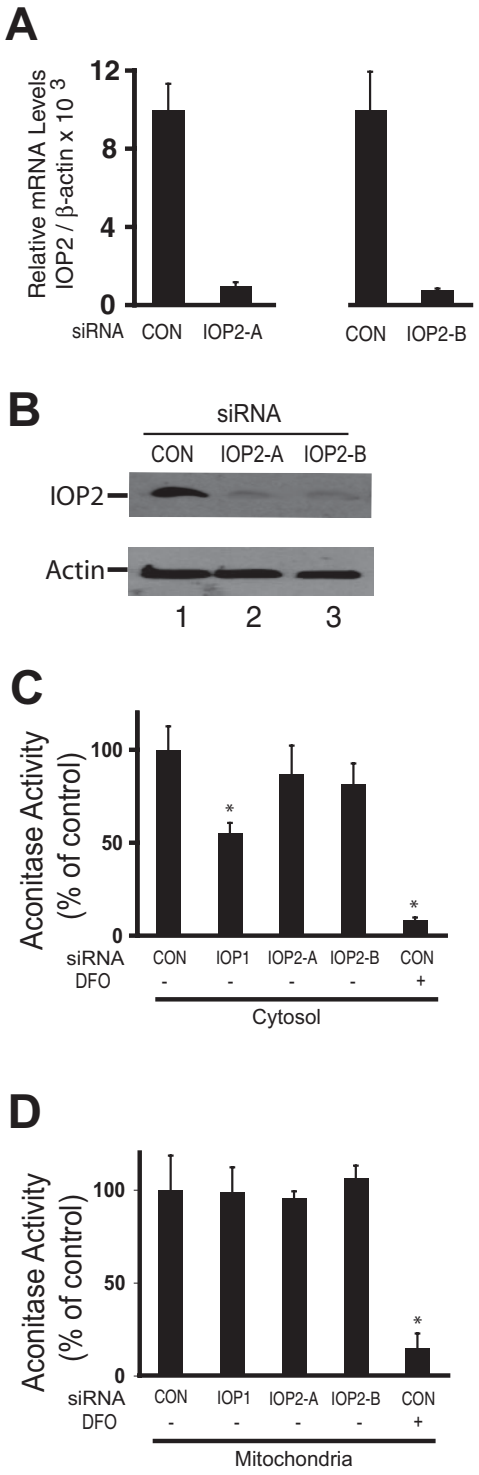

FIGURE 4. **Comparison of IOP1 and IOP2 knockdown on aconitase activity in HeLa cells.** HeLa cells were transfected with the indicated siRNAs. *A*, total RNA was isolated from cells and analyzed by real-time PCR for IOP2 mRNA (means ± S.D.) and normalized to that of β-actin. The levels of IOP2 mRNA following IOP2-A or IOP2-B siRNA treatment are 13 and 11% of control, respectively. *B*, extracts (20 μg) were analyzed by Western blotting using antibodies against IOP2 or actin, as indicated. *C–D*, cytosolic or mitochondrial extracts were assayed for aconitase activity. Some cells were also treated with 100 μM DFO for 20 h prior to harvest, as indicated. Shown are the means ± S.D., $n = 3$. *, $p < 0.01$.

treatment almost completely abolished aconitase activity in both cytosolic and mitochondrial extracts (Fig. 4, *C* and *D*). These results indicate, at a minimum, that IOP1 and IOP2 are not identical in function and furthermore provide evidence that IOP1 plays a more important role among the two IOP isoforms in cytosolic Fe-S protein biogenesis.

A distinctive feature of cytosolic aconitase is that upon loss of its active Fe-S cluster it converts to IRP1, an RNA-binding protein that binds to specific stem loop structures known as iron-response elements (IRE) (26, 27). These IREs are located in 5′- and 3′-untranslated regions (UTRs) of select mRNAs that are involved in various aspects of iron metabolism. For example, multiple tandem IREs are located in the 3′-UTR of TfR1, and binding of IRP1 to the 3′-UTR IRE results in increased stability and therefore increased half-life of the TfR1 mRNA. A different IRE is located in the 5′-UTR of the ferritin heavy chain mRNA, and binding of IRP1 to this IRE has a different effect, namely, inhibition of protein translation. In this manner, IRP1 plays an important role in adaptive responses to iron deprivation through its up-regulation of TfR1, which promotes the uptake of iron into cells, and its down-regulation of ferritin, which promotes the release of intracellular iron stores.

We examined whether impairment of Fe-S protein biogenesis affects IRP activity. We knocked down IOP1 in HeLa cells. We then transfected them with a luciferase reporter construct in which the IRE-containing 3′-UTR of the TfR1 gene was subcloned into the 3′-UTR of the luciferase gene and subsequently measured luciferase activity. DFO, by virtue of chelating the active site iron, would be expected to convert cytosolic aconitase to IRP1, and consistent with this, it activates the reporter gene (Fig. 5*A*). Importantly, we also found that IOP1 knockdown activates the 3′-IRE reporter gene as well. In parallel experiments, we also harvested mRNA, performed reverse transcription, and then conducted real-time PCR to measure endogenous TfR1 message. As shown in Fig. 5*B* and supplemental Fig. S3, TfR1 message is also increased by IOP1 knockdown. The difference in the magnitude of the effect of IOP1 knockdown in Fig. 5, *A* and *B*, may relate to the fact that regulatory elements do not behave exactly like their endogenous counterparts when taken out of their natural context. For example, the transferrin receptor iron-response element can show varying degrees of potency depending on the reporter system employed (28).

We performed experiments to examine effects of IOP1 knockdown on ferritin heavy chain protein levels. Cells were treated with siRNA and then cytosolic extracts prepared and examined by Western blotting. As shown in Fig. 5*C*, under conditions where NFS1 knockdown decreases ferritin heavy chain protein expression, we found that IOP1 does so as well, although not perhaps as dramatically. Real-time PCR shows that the change in ferritin heavy chain protein level cannot be attributed to changes in mRNA level (Fig. 5*D*). The changes also cannot be attributed to changes in protein levels of IRP2 (Fig. 5*C*), which can also bind to IREs but unlike IRP1 does not possess an Fe-S cluster. The results, in turn, are consistent with increased IRP1 activity.

To further examine this, we prepared a radiolabeled IRE probe derived from the ferritin heavy chain 5′-UTR and employed it in an IRP electrophoretic mobility shift assay. Incubation of the probe with HeLa cell cytoplasmic extracts results in electrophoretic mobility shift (Fig. 5*E*). This shift is indistin-

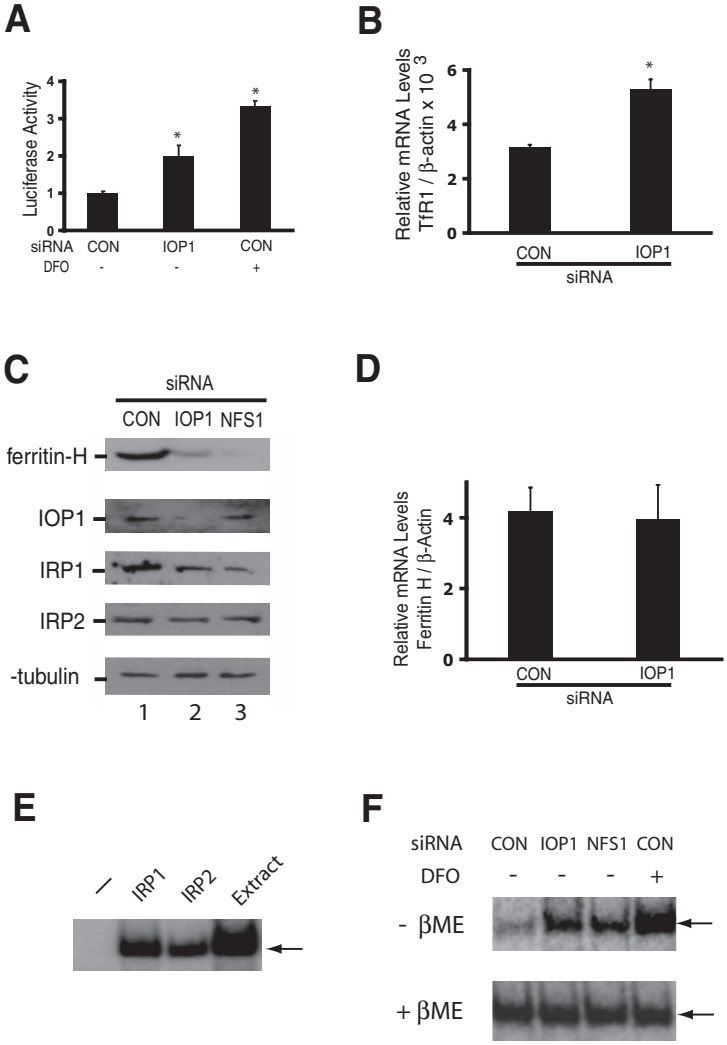

FIGURE 5. **Effects of IOP1 knockdown on IRP targets.** *A* and *B*, HeLa cells were transfected with the indicated siRNA. On day 7, cells were also cotransfected with pIRE3-Luc and pRL-TK, and 48 h later, luciferase activities were measured (*A*) and total RNA extracted and measured for TfR1 mRNA levels by real-time PCR (*B*). In *A*, firefly luciferase activity was normalized to that of *Renilla* luciferase. In *B*, TfR1 mRNA levels were normalized to that of β-actin. The level of TfR1 mRNA upon IOP1 knockdown is 165% of that of control. *, $p < 0.01$. *C–E*, HeLa cells were transfected with the indicated siRNA. *C*, cytosolic extracts (20 μg) were subjected to Western blotting with the indicated antibodies. Shown is one of two to three representative experiments. *D*, total RNA was isolated from cells and analyzed by real-time PCR for ferritin heavy chain mRNA (means ± S.D.) and normalized to that of β-actin. Essentially the same result was obtained employing a second independent set of real-time PCR primers for ferritin heavy chain mRNA (data not shown). *E*, a ^{32}P-labeled RNA probe containing the ferritin heavy chain 5′-IRE was incubated with or without immunopurified IRP1 or IRP2 or HeLa cell cytoplasmic extract as indicated and then subjected to 5% PAGE. *Arrow* indicates IRP gel shift. *F*, cytosolic extracts (2 μg) were incubated with a ^{32}P-labeled RNA probe containing the ferritin heavy chain 5′-IRE and subjected to 5% PAGE. In some samples, 2% β-mercaptoethanol (*βME*) was included in the incubation. *Arrows* indicates IRP gel shift. One of three representative experiments is shown.

guishable from that induced by either immunopurified IRP1 or IRP2, thereby providing evidence that this shift reflects IRP activity. We note that human IRP1 and IRP2 produce indistinguishable shifts in this assay, consistent with previous reports (29). We then examined cytoplasmic extracts from siRNA-treated HeLa cells. Under conditions in which NFS1 knockdown results in increased IRP activity, as shown previously (11), we found that IOP1 knockdown does so as well (Fig. 5*F*). Treatment of extracts with β-mercaptoethanol, an agent that activates IRP, results in increased gel shift signals for all samples. The increased IRP activity cannot be accounted for by increases in IRP1 protein levels (Fig. 5*C*). In fact, IOP1 knockdown results in slightly decreased IRP1 levels, as does NFS1 knockdown. This NFS1 knockdown-associated decrease has previously been reported by others (11), and others have also reported that apo-IRP1 is less stable than the holoenzyme (30, 31). The gel shift results also cannot be accounted for by IRP2, because levels of this protein are not appreciably changed. IRP1 is regulated by loss of its active site iron and does not necessarily have to be accompanied by increases in protein level, as opposed to IRP2, which is regulated at the level of protein stability (32). Indeed, conversion of only a small fraction of IRP1 from iron-sulfur-replete to iron-sulfur-deficient forms is sufficient to result in significant IRE binding activity (33), and the results observed are therefore consistent with increased IRP1 RNA binding activity. This, in turn, is consistent with the decreased cytosolic aconitase activity observed in the earlier experiments.

DISCUSSION

The biogenesis of cytosolic Fe-S proteins in eukaryotes has received substantial recent attention, and it is clear that we are far from a complete understanding of this essential process (2). The present results provide evidence for a role for IOP1 in the mammalian pathway. Knockdown of IOP1 results in impaired cytosolic aconitase and xanthine oxidase activities, and we also provide evidence for increased IRP1 activity. IOP1 knockdown did not impair mitochondrial aconitase activity nor did it impair the activities of non-Fe-S proteins, suggesting a specific role for IOP1 in cytosolic Fe-S protein biogenesis. We also did not find evidence for involvement of IOP2 in cytosolic Fe-S protein biogenesis. IOP2 is a nuclear protein, and we cannot rule out the possibility that in addition to its role in binding prenylated prelamin A in the nuclear membrane, IOP2, or for that matter IOP1, may have a role in the biogenesis of nuclear, as opposed to cytosolic, Fe-S proteins.

In *S. cerevisiae*, four essential proteins involved in Fe-S protein biogenesis have been identified, Cfd1, Nbp35, Cia1, and Nar1. IOP1 is homologous to the latter, and this therefore provides evidence that the Fe-S pathway in yeast may be conserved in mammals. Further studies are needed to determine whether homologues of the other yeast proteins exist in mammals, and if

so, whether they fulfill essential functions in cytosolic Fe-S protein biogenesis. That being said, these results do not rule out a potential role for other pathways, such as ones employing cytosolic versions of otherwise predominantly mitochondrial proteins, in the biogenesis of cytosolic Fe-S proteins. We observed that knockdown of IOP1 in HeLa cells impaired growth and inhibited global protein synthesis. As deletion of Nar1 in *S. cerevisiae* is lethal and linked to the maturation of Rli1p, an essential cytosolic Fe-S protein required for ribosome biogenesis (24, 25), it will be of interest to determine whether these IOP1 knockdown-associated effects in mammalian cells might involve a similar pathway.

We had previously identified IOP1 as a modulator of HIF-1α activity (15). Specifically, knockdown of IOP1 in Hep3B cells was found to up-regulate HIF-1α mRNA and protein levels. HIF-1α is a master regulator of the hypoxic response, transcriptionally up-regulating genes involved in glucose uptake, glycolysis, and angiogenesis, among others, that allow cells to survive oxygen deprivation (17). These considerations might raise the possibility that up-regulation of HIF-1α may be mediated by the cytosolic Fe-S pathway. However, we note that NFS1 knockdown, which impairs cytosolic aconitase activity, did not affect HIF-1α protein levels (data not shown). This therefore suggests that IOP1 modulation of HIF-1α may occur independent of its role in cytosolic Fe-S protein biogenesis. At the same time, it also does not rule out the possibility of other Fe-S pathway-dependent effects of IOP1 on the hypoxia pathway. In this regard, an IRE has been identified in the 5′-UTR of the transcript of a different HIF-α isoform, HIF-2α (34), thereby providing a potential link between IOP1, the cytosolic Fe-S protein pathway, and the hypoxic response. Iron in the presence of oxygen can generate reactive oxygen species, and oxygen itself can directly damage Fe-S clusters, emphasizing the need to have proper coordination between the iron and oxygen homeostatic pathways.

An important consideration in these as well as previous siRNA studies is that knockdown is not 100% efficient. Thus, effects may only be observed after protein levels are reduced below a critical level necessary for function, and this may vary in both a gene-specific and cell type-specific manner. Indeed, this may account for the fact that dimunition of aconitase and xanthine oxidase activities is partial, as opposed to complete, following IOP1 knockdown in the present studies. These considerations also make it important to consider other approaches, such as gene knock-out approaches, in evaluating the roles of these intriguing proteins.

Acknowledgments—We thank Drs. Celeste Simon and Liping Liu for help with the protein synthesis assays and Drs. Zissimos Mourelatos and Robert Wilson for advice with the IRP gel shift assays.

REFERENCES

1. Johnson, D. C., Dean, D. R., Smith, A. D., and Johnson, M. K. (2005) *Annu. Rev. Biochem.* **74,** 247–281
2. Lill, R., and Muhlenhoff, U. (2006) *Annu. Rev. Cell Dev. Biol.* **22,** 457–486
3. Lill, R., and Muhlenhoff, U. (2005) *Trends Biochem. Sci.* **30,** 133–141
4. Roy, A., Solodovnikova, N., Nicholson, T., Antholine, W., and Walden, W. E. (2003) *EMBO J.* **22,** 4826–4835
5. Hausmann, A., Aguilar Netz, D. J., Balk, J., Pierik, A. J., Muhlenhoff, U., and Lill, R. (2005) *Proc. Natl. Acad. Sci. U. S. A.* **102,** 3266–3271
6. Balk, J., Aguilar Netz, D. J., Tepper, K., Pierik, A. J., and Lill, R. (2005) *Mol. Cell. Biol.* **25,** 10833–10841
7. Balk, J., Pierik, A. J., Netz, D. J., Muhlenhoff, U., and Lill, R. (2004) *EMBO J.* **23,** 2105–2115
8. Netz, D. J., Pierik, A. J., Stumpfig, M., Muhlenhoff, U., and Lill, R. (2007) *Nat. Chem Biol.* **3,** 278–286
9. Rouault, T. A., and Tong, W. H. (2005) *Nat. Rev. Mol. Cell Biol.* **6,** 345–351
10. Biederbick, A., Stehling, O., Rosser, R., Niggemeyer, B., Nakai, Y., Elsasser, H. P., and Lill, R. (2006) *Mol. Cell. Biol.* **26,** 5675–5687
11. Fosset, C., Chauveau, M. J., Guillon, B., Canal, F., Drapier, J. C., and Bouton, C. (2006) *J. Biol. Chem.* **281,** 25398–25406
12. Li, K., Tong, W. H., Hughes, R. M., and Rouault, T. A. (2006) *J. Biol. Chem.* **281,** 12344–12351
13. Tong, W. H., and Rouault, T. A. (2006) *Cell Metab.* **3,** 199–210
14. Tong, W. H., Jameson, G. N., Huynh, B. H., and Rouault, T. A. (2003) *Proc. Natl. Acad. Sci. U. S. A.* **100,** 9762–9767
15. Huang, J., Song, D., Flores, A., Zhao, Q., Mooney, S. M., Shaw, L. M., and Lee, F. S. (2007) *Biochem. J.* **401,** 341–352
16. Barton, R. M., and Worman, H. J. (1999) *J. Biol. Chem.* **274,** 30008–30018
17. Semenza, G. L. (1999) *Annu. Rev. Cell Dev. Biol.* **15,** 551–578
18. Yu, F., White, S. B., Zhao, Q., and Lee, F. S. (2001) *Cancer Res.* **61,** 4136–4142
19. Drapier, J. C., and Hibbs, J. B., Jr. (1996) *Methods Enzymol.* **269,** 26–36
20. Setchenska, M. S., and Arnstein, H. R. (1978) *Biochem. J.* **170,** 193–201
21. Liu, L., Cash, T. P., Jones, R. G., Keith, B., Thompson, C. B., and Simon, M. C. (2006) *Mol. Cell* **21,** 521–531
22. Mueller, S., and Pantopoulos, K. (2002) *Methods Enzymol.* **348,** 324–337
23. Henderson, B. R., Seiser, C., and Kuhn, L. C. (1993) *J. Biol. Chem.* **268,** 27327–27334
24. Yarunin, A., Panse, V. G., Petfalski, E., Dez, C., Tollervey, D., and Hurt, E. C. (2005) *EMBO J.* **24,** 580–588
25. Kispal, G., Sipos, K., Lange, H., Fekete, Z., Bedekovics, T., Janaky, T., Bassler, J., Aguilar Netz, D. J., Balk, J., Rotte, C., and Lill, R. (2005) *EMBO J.* **24,** 589–598
26. Hentze, M. W., Muckenthaler, M. U., and Andrews, N. C. (2004) *Cell* **117,** 285–297
27. Rouault, T. A. (2006) *Nat. Chem. Biol.* **2,** 406–414
28. Casey, J. L., Hentze, M. W., Koeller, D. M., Caughman, S. W., Rouault, T. A., Klausner, R. D., and Harford, J. B. (1988) *Science* **240,** 924–928
29. Guo, B., Brown, F. M., Phillips, J. D., Yu, Y., and Leibold, E. A. (1995) *J. Biol. Chem.* **270,** 16529–16535
30. Clarke, S. L., Vasanthakumar, A., Anderson, S. A., Pondarre, C., Koh, C. M., Deck, K. M., Pitula, J. S., Epstein, C. J., Fleming, M. D., and Eisenstein, R. S. (2006) *EMBO J.* **25,** 544–553
31. Wang, J., Fillebeen, C., Chen, G., Biederbick, A., Lill, R., and Pantopoulos, K. (2007) *Mol. Cell. Biol.* **27,** 2423–2430
32. Eisenstein, R. S. (2000) *Annu. Rev. Nutr.* **20,** 627–662
33. Meyron-Holtz, E. G., Ghosh, M. C., Iwai, K., LaVaute, T., Brazzolotto, X., Berger, U. V., Land, W., Ollivierre-Wilson, H., Grinberg, A., Love, P., and Rouault, T. A. (2004) *EMBO J.* **23,** 386–395
34. Sanchez, M., Galy, B., Muckenthaler, M. U., and Hentze, M. W. (2007) *Nat. Struct. Mol. Biol.* **14,** 420–426